Astro2020 APC White Paper

The Next Generation Magnetic Spectrometer in Space: An International Science Platform for Physics and Astrophysics at Lagrange Point 2

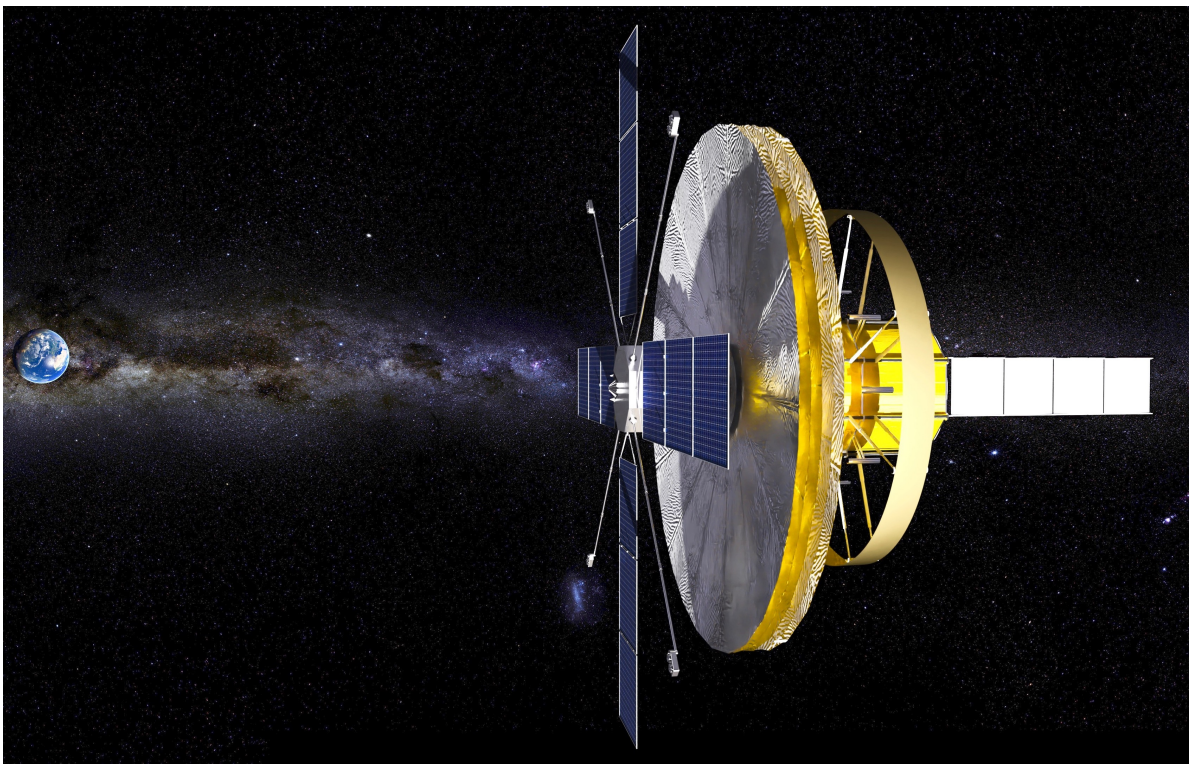

Consideration Area:
Space-Based Project (Large)

Authors:
S.P. Wakely (Chicago), S. Schael (RWTH Aachen), A. Bay (EPF Lausanne), J.J. Beatty (Ohio State), J. Berdugo (CIEMAT), J.H. Buckley (WashU), D. Caprioli (Chicago), S. Coutu (Penn State), P. von Doetinchem (Hawaii), H. Gast (RWTH Aachen), B. Heber (CAU Kiel), P.S. Marrocchesi (Siena), P. Mertsch (RWTH Aachen), I. Moskalenko (Stanford), D. Müller (Chicago), J. Musser (Indiana), S. Nutter (N. Kentucky), R.A. Ong (UCLA), N. Park (UW Madison), T.A. Porter (Stanford), C. Senatore (Geneva), L. Shchutska (EPF Lausanne)

Contact:
Name: Scott P. Wakely
Institution: University of Chicago
Email: wakely@ulysses.uchicago.edu

1 Introduction

The past decade has witnessed a remarkable explosion of dramatic paradigm-challenging results in particle astrophysics. The most impactful of these results have emerged from a new generation of high-precision space-based instruments, such as PAMELA[1], AMS-02[2], and Fermi/LAT[3]. These instruments – in particular, the magnetic spectrometers PAMELA and AMS-02 – have revealed unexpected features in the cosmic-ray matter and antimatter flux spectra that have challenged much of our traditional understanding of particle astrophysics, across a range of topics. These topics include questions of cosmic-ray origins, high-energy particle acceleration and propagation mechanisms, and the nature of dark matter. Perhaps the most intriguing result has been the recent observation of a few candidate cosmic-ray anti-helium events[4], which, if confirmed, would have profound implications for our understanding of the matter-antimatter asymmetry of the universe.

Addressing these questions, and extending current measurements to higher energies, requires powerful new instrumentation with extended exposure times. And while pure calorimeters, such as the presently deployed DAMPE[5] and CALET[6] can provide some answers, only magnetic spectrometers, with their ability to differentiate charge sign, and even measure particle mass, can properly address the full scope of open questions.

The project described in this white paper is a next-generation spectrometer (referred to as NGS throughout) conceived to be an international platform for precision particle astrophysics and fundamental physics, at energy scales well beyond the reach of all current detector payloads. Achieving this will require overcoming a number of key technical challenges, though in many cases, technology already exists that can be adapted to provide the needed performance.

The heart of the instrument is a thin, large-volume high-temperature superconducting (HTS) solenoid magnet, which provides a uniform 1T field within the tracking volume. When instrumented with proven silicon-strip and scintillating fiber technologies, the spectrometer will achieve a maximum detectable rigidity (MDR, defined by $\sigma_R/R = 1$) of 100 TV, with an effective acceptance of 100 m^{2}sr. A deep ($70\,X_0/4\,\lambda_I$) central calorimeter will provide energy measurements and particle identification, with innovative 'cubic' detector elements enabling a large acceptance of 30 m^{2}sr.

Combined, this instrumentation will vastly improve on existing measurements and allow us to probe, with high statistics and high precision, the positron and electron spectra to 10 TeV, the antiproton spectrum to 10 TeV, the anti-deuteron spectrum to 8 GeV/n, and the nuclear cosmic-ray component to 10^{16} eV, past the cosmic-ray knee. At the same time, it will greatly expand our sensitivity to heavy cosmic antimatter ($Z \leq -2$), and provide all-sky coverage for very-high-energy gamma rays with excellent resolution and energy reach. The magnet and detector systems will be designed with no consumables, allowing for an extended 10-year payload lifetime at its thermally-favorable orbital location at Sun-Earth Lagrange Point 2 (L2).

This white paper draws heavily on a recently submitted design study[7], which contains considerably more detail than can be fit into this format. The goal here is to simply introduce the mission scope and goals and advocate for support over the next decade.

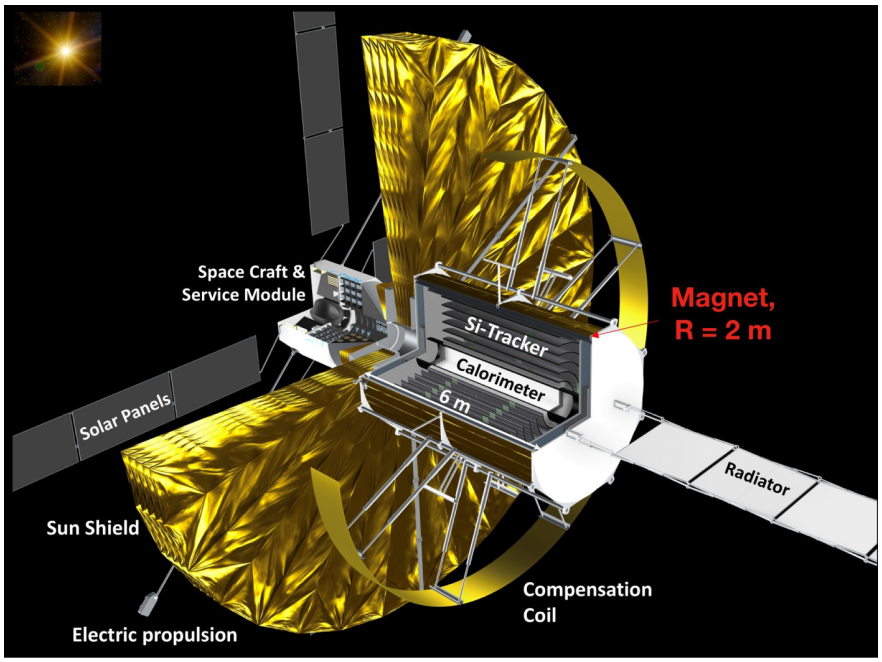

Figure 1: NGS Detector Concept

2 Key Science Goals and Objectives

NGS is conceived as a wide-focus platform for precision high energy astrophysics and physics across a broad range of topics. The size, variety, and sensitivity of its instrumentation are chosen to allow it to address key open questions in particle astrophysics, make important contributions to multi-messenger astrophysics, and open a large window of discovery space. In addition to the topics discussed in more detail below, the science possible with NGS includes studies of cosmic particle and gamma-ray anisotropies, measurements of various isotopes and heavy (trans-iron) nuclei in cosmic rays, searches for exotic particles, such as strangelets [8], magnetic monopoles [9], and fractionally-charged particles [10], searches for evaporating primordial black holes [11, 12], and investigations of quantum gravity through precision energy/arrival-time measurements of photons from γ-ray bursts [13]. In the following, detector acceptances have been calculated using GEANT4[14].

2.1 Protons and Other Nuclei

Protons are the most abundant species in cosmic rays. PAMELA and AMS-02 have reported unexpected spectral breaks above ~ 200 GV in the spectra of protons and other light nuclei [15–17]. Such spectral breaks encode information about the sources and propagation history of cosmic rays, but thus far, no coherent and well-accepted description of the various observed features has emerged. NGS will have the size and energy reach to directly measure, for the first time ever, light nuclei in cosmic rays up to and through the energy of the cosmic-ray knee, as well as heavier nuclei with vastly improved statistics. The detailed spectral and composition studies enabled by NGS through the knee region will directly address several unresolved decades-old questions in cosmic-ray astrophysics including, for instance, what is the maximum energy that can be reached by galactic cosmic-ray accelerators. This information also forms an essential context for the

other studies detailed below, such as the origin of cosmic-ray positrons, electrons, antiprotons, and antimatter.

2.2 Positrons and Electrons

The unexpected excess of high-energy positrons observed above the predicted yield from cosmic-ray collisions has been one of the most exciting developments in high-energy astrophysics in the last generation. As measured by AMS-02, the flux shows a dramatic rise at ~ 20 GeV, followed by a sharp spectral break downward at ~ 300 GeV[18]. Possible interpretations have ranged from new effects in cosmic-ray acceleration and propagation [19–21], to new astrophysical sources such as pulsars [22–30], to dark matter decay or annihilation [31–39]. A generic source term, which describes the contribution of the new source responsible for the positron excess, can be described by a power law with an exponential cutoff (see, e.g., [18]). NGS will have the size and energy reach required to measure, with very high statistics, the intermediate energies of 100-1000 GeV in the cosmic-ray electron spectrum, as well as to completely map out the region up to and beyond the cutoff energy. This region may include features associated with local sources of primary electrons/positrons predicted in propagation models. Identifying such features will shed light onto the origin of positrons, electrons, and other cosmic-ray species. Measurements up to ~ 20 TeV should be achievable with high statistics, an order of magnitude higher than existing detectors. - see Figure2.

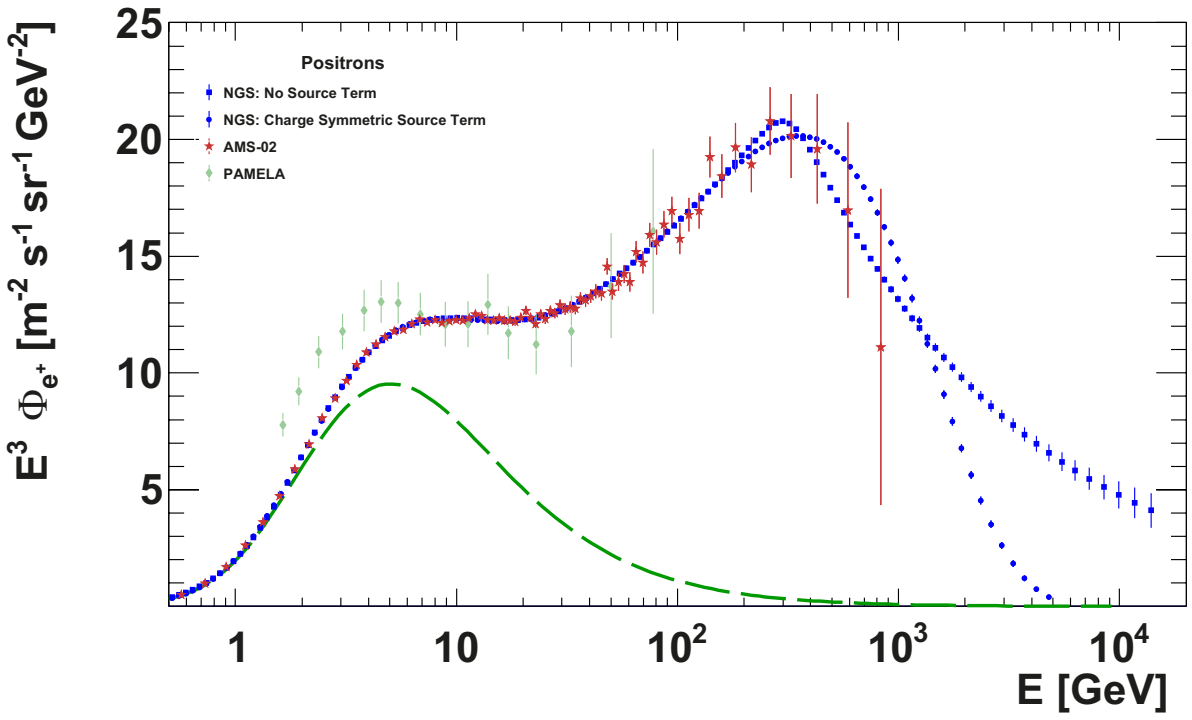

Figure 2: Cosmic-ray positron spectrum. Expected data from NGS (statistical errors only) for two different scenarios: a) Blue Circles: a power law spectrum plus a source term with exponential cutoff - see text. b) Blue squares: generic multiple power law with spectral breaks, with the last break at 300 GeV. The dashed green curve shows the expected spectrum from a) without the source term. Recent experimental data from PAMELA [40] and AMS-02 [18] are shown.

If the origin of the positron source term is a process that also produces electrons in equal amounts, then there should also be a signature detectable in the cosmic-ray electron spectrum. Both pulsar models and dark matter models generically predict such a charge-symmetric source term, but current detectors lack the statistics and energy reach needed to unambiguously identify such signatures. At higher energies, H.E.S.S. [41], VERITAS[42], and DAMPE [43] have observed a spectral break in the combined electron and positron flux at about ~ 1 TeV, which might be related to this question, though firm conclusions are hampered by a lack of statistics. NGS will have the size and energy reach required to measure, with very high statistics, the intermediate energies of 100-1000 GeV in the cosmic-ray electron spectrum, as well as to completely map out the region up to and beyond the cutoff energy. Measurements to ~ 20 TeV with high statistics should be achievable, an order of magnitude higher than existing detectors.

2.3 Antiprotons and Antihelium

A key discriminator between various positron origin models is the presence or lack of antiprotons. While pulsars will not generate these antiparticles, most dark matter origin models do. Hence, a signature of these models is often a companion anomaly in the cosmic-ray antiproton flux, unless the dark matter couples predominantly to leptons. NGS will be able to measure the antiproton spectrum to energies more than an order of magnitude above current detectors, providing precise information on the spectral shape up to up ~ 10 TeV.

AMS-02 has shown in 2018 both $^3\overline{\mathrm{He}}$ and $^4\overline{\mathrm{He}}$ candidate events at a CERN Colloquium [4]. These unexpected events are observed in AMS-02 at a rate of 1 event/year or 1 $\overline{\mathrm{He}}$ event per 100 million He events, well above the rate of secondary $\overline{\mathrm{He}}$ production in coalescence models. Their origin is presently unclear, however, the statistically significant detection of unambiguous anti-helium events could have the most profound implications for physics and astrophysics. Progress in this direction requires new instrumentation achieving high-confidence particle identification, a solid understanding of potential backgrounds, and powerful systematic checks. NGS will have the performance and exposure to do exactly this - extrapolating the AMS-02 candidate $\overline{\mathrm{He}}$ event rate to the NGS acceptance results in the prediction of $\sim 1000\overline{\mathrm{He}}$ events/year. Additionally, the rotational symmetry of NGS allows systematic studies equivalent to inverting the magnetic field of the detector. As AMS-02 has demonstrated [44], cosmic-ray nuclei belong to one of only two families: primary or secondary cosmic-ray nuclei, each with distinctive spectral shape. Hence, the precision measurement of the spectral shape of the $\overline{\mathrm{He}}$ flux will allow key tests of the origin of $\overline{\mathrm{He}}$.

2.4 Antideuterons

Antideuterons potentially are the most sensitive probe for dark matter in the cosmic rays [50, 51]. While antiprotons are dominantly produced in secondary interactions in the interstellar medium, antideuterons at low energy have no other known origin. No antideuterons have ever been identified in cosmic rays. The current best limit has been set by BESS [52], excluding a flux of $1.9 \times 10^{-4}\,(\mathrm{m^2\,s\,sr\,GeV/n})^{-1}$ between 0.17 GeV/n and 1.15 GeV/n at the 95 % confidence level, though results from more sensitive searches at low energy are expected from both AMS-02 and GAPS in the next few years. The expected sensitivity of NGS is $3 \times 10^{-11}\ (\mathrm{m^2\,s\,sr\,GeV/n})^{-1}$ in the energy range between 0.1 GeV/n and 8 GeV/n. At this level of sensitivity, it is no longer useful to quote an *integral* sensitivity, which is related to the chances of observing a certain number of events *anywhere* inside a given energy range. Instead, we calculate a *differential* sensitivity,

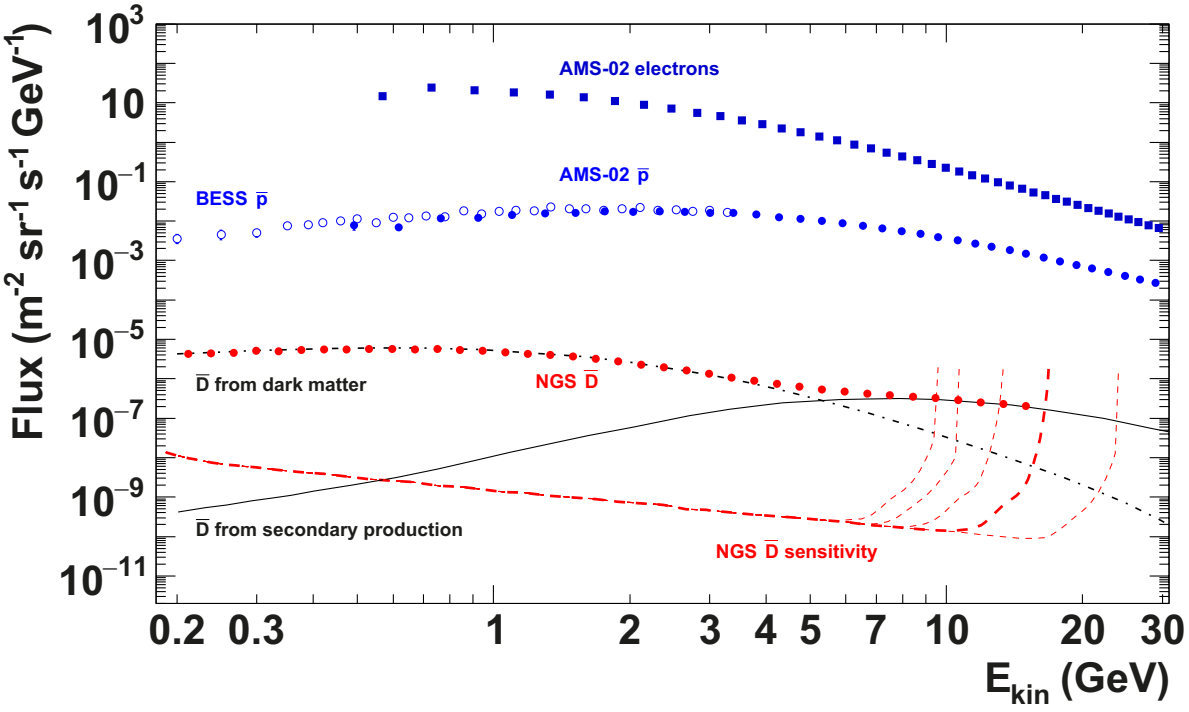

Figure 3: Differential sensitivity of NGS to antideuterons in cosmic rays for a mission time of 10 years and a single-layer ToF time resolution of 20 ps, with a logarithmic binning of 20 bins per decade (thick dashed red curve). Sensitivities for time resolutions of 10 ps, 30 ps, 40 ps and 50 ps are shown by thin dashed red curves (from right to left). The red symbols show the expected data from NGS if the antideuteron flux follows the dark matter model of Ref. [45] with statistical uncertainties (which are smaller than the symbol size). The solid black curve shows the antideuteron flux expected from secondary production by charged cosmic rays interacting with the interstellar material, as derived in Ref. [46] for the EPOS LHC interaction model. Data for the other $Z = -1$ particles in cosmic rays, from AMS-02 [47, 48] and BESS-Polar [49], are shown to indicate the signal to background ratios for the antideuteron measurement.

which can be directly compared to model predictions for the differential $\bar{D}$ flux. We choose a logarithmic energy binning with 20 bins per decade and calculate the sensitivity individually for each bin. The differential sensitivity for antideuterons is shown in Fig. 3. It is defined as the 95 % CL limit that will be set in case no $\bar{D}$ events are observed in the given bin. NGS will be the first instrument to measure the cosmic-ray antideuteron spectrum with thousands of events, even in the pessimistic case that antideuterons originate only from secondary production. NGS will have the sensitivity to distinguish between antideuterons originating in dark matter annihilations and those produced in interactions within the interstellar medium, due to the different spectral shapes expected for these components. While it is not clear if antideuterons from dark matter annihilation exist, the observation of antideuterons from secondary production would allow us to set additional constraints on the $^{3}\overline{\mathrm{He}}$ and $^{4}\overline{\mathrm{He}}$ rates in cosmic rays: Every nucleon in the antimatter particle reduces the production rate by a factor $\simeq 10^{3} - 10^{4}$ depending on the energy, i.e. we expect $N(\bar{p}) : N(\bar{D}) : N(^{3}\overline{\mathrm{He}}) : N(^{4}\overline{\mathrm{He}}) \approx 1 : 10^{-3} - 10^{-4} : 10^{-6} - 10^{-7} : 10^{-9} - 10^{-10}$ in cosmic rays if there is no new source for one of these antimatter species [53]. A simultaneous

measurement of these sensitive probes for new physics is therefore required to derive a coherent picture.

2.5 Gamma-ray Measurements

NGS will allow detailed studies of γ-ray sources [54] and the diffuse γ-ray up to the ~ 10 TeV scale due to its large 60 m^2 sr acceptance for γ rays. This acceptance results partially from the reconstruction of photons in the calorimeter (30 m^2 sr), with a similar contribution from photon conversions in the thin main solenoid. The angular resolution for converted photons is limited by multiple scattering of the resulting electron-positron pairs at low energies, but at high energies, the direction of the photon can be reconstructed with high accuracy due to the good spatial resolution and long lever arm of the silicon tracker. This will allow, for example, the imaging of features in sources such as supernova remnants [55, 56] and pulsar wind nebulae[57] with resolution similar to today's best X-ray telescopes.

Far from the shadow of the Earth, NGS will monitor most of the sky continuously. For example, it does not have to be rotated to be sensitive to, e.g. γ-ray bursts or photons emitted in conjunction with gravitational wave events. It will therefore also provide a background measurement for sky regions where transient sources are observed. In combination with ground-based experiments, it will participate in multi-messenger networks for modern astronomy, which combine detectors for gravitational waves, cosmic-ray neutrinos and cosmic γ rays. In particular, NGS can serve as a trigger for the Cherenkov Telescope Array [58] and similar ground-based observatories for the detailed follow-up investigation of transient sources.

3 Technical Overview and Technology Drivers

Achieving the science goals described above requires an ambitious detector design to dramatically improve on the current state-of-the-art in sensitivity, precision, and energy reach. For instance, the spectrometer must maintain a very large geometric factor of 100 m^2sr, and a high MDR (100 TV), while retaining good resolution at low rigidity. This implies a large high-field magnet, with excellent tracking resolution and a small material budget to avoid multiple scattering. The long exposure times needed for statistical accuracy require that all systems be capable of extended operation in space, which excludes the use of cryogens for magnet cooling, implying high-temperature superconductors and advanced thermal designs. For the calorimeter to simultaneously achieve the required geometric factor and depth for high-energy particles, new concepts in 3D shower reconstruction should be pursued. Other systems will be required to achieve very high performance levels, such as time-of-flight counters, where excellent ($\mathcal{O}$(10 ps)) timing resolution is required to enable isotope separation.

Fortunately, much of the technology required for NGS can be adapted or developed from detector systems in existing or near-future instruments. However, there will be challenges in achieving the required system scales and performance levels, as well as in adapting components to long-term stable deployment in space. Below we identify plausible candidate options for these systems and discuss technology drivers that will require near-term R&D efforts.

3.1 Magnet Design

To achieve the desired performance specifications, the NGS solenoid magnet must have a thin wall, a length of 6m and a diameter of 4m, while achieving a uniform central field of 1T. To

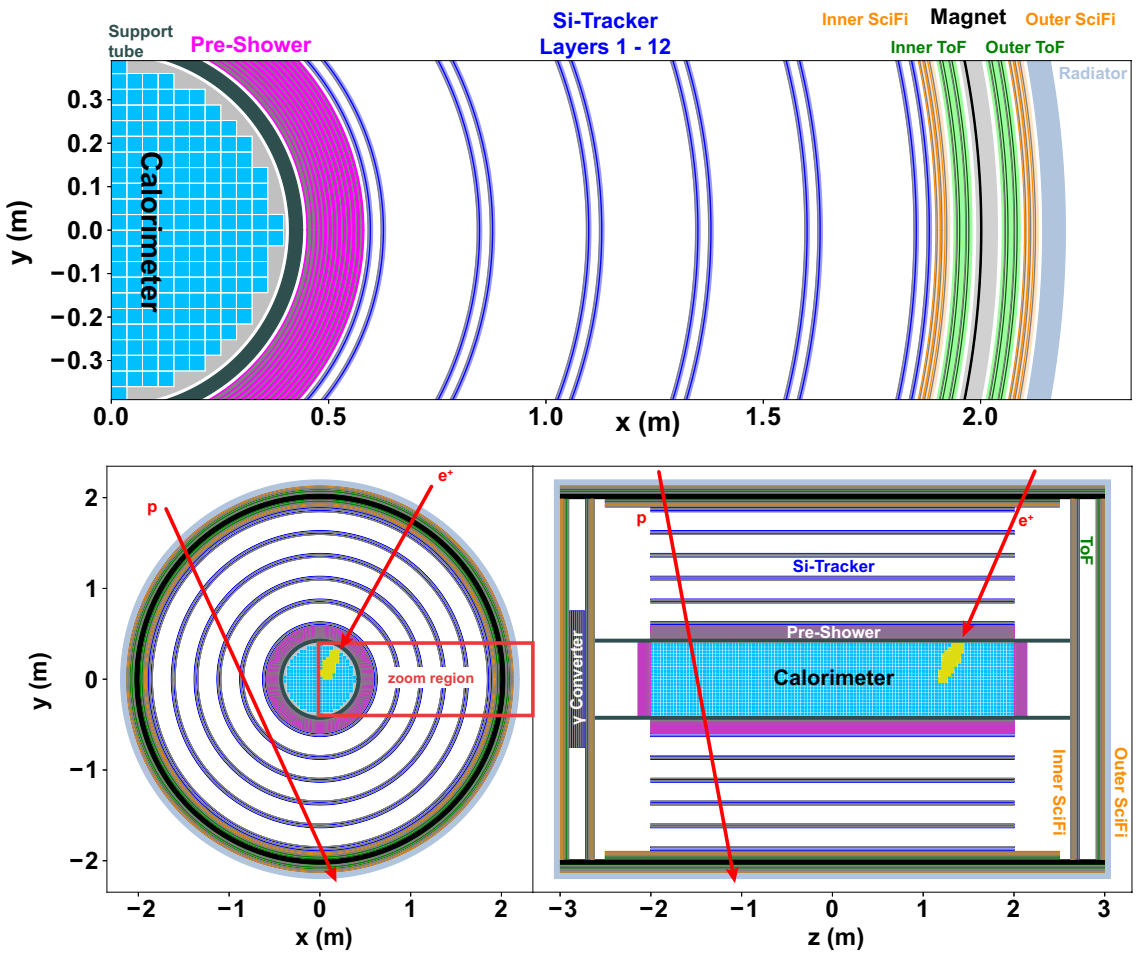

Figure 4: Schematic view of the NGS instrument and its response to protons and positrons. The magnetic field inside the inner solenoid is oriented in the z-direction, i.e., the left view shows the bending plane of the magnet, and a transverse view is shown on the right. The upper panel shows a zoom into the xy view.

provide superconducting operation for a 10-year period without consumable cryogens, construction from high-temperature superconducting (HTS) materials is required. This will allow the magnet to operate, behind a sun shield, using only radiative cooling to deep space. Thermal models indicate that temperatures of 40K-50K can be achieved, which still leaves some margin for conductive thermal loads from other detector or spacecraft elements. Similar to JWST, this thermal configuration requires NGS to be located in a stable, cold environment, such as Lagrange Point 2.

Second-generation (2G) HTS wire made from rare-earth barium copper oxide (REBCO) material[59, 60] is a promising option for the solenoid winding. HTS wire can carry high current densities even at field strengths of 30 T[61] and can tolerate severe mechanical stresses[62, 63] when paired to $30-75$ μm Hastelloy substrates. Recently, 2G REBCO wire has become available in extended lengths (450m) that has been demonstrated to operate (at T=50K) with critical current densities better than required for the baseline magnet design of 22 layers of 12mm-wide wire at 500A[64].

In addition to the main solenoid, NGS will be outfitted with a superconducting compensation magnet, in the form of a 1.2m-wide coil of 12m diameter, located at the midpoint of the solenoid. The purpose of the compensation magnet is to cancel out the magnetic dipole moment of the main coil, without which even the weak, ~ 10 nT interplanetary magnetic fields at L2 will be sufficient to impart an overly large ($\sim 10^6$ N m s) angular momentum to the payload, over the course of a year.

It has never been demonstrated that a HTS magnet with a lightweight support structure can be operated in space. In particular, vibrations during launch are a concern. Other key areas for research include improved understanding of quench dynamics[65] in HTS wire, and the design and testing of appropriate quench protection systems. Also, because the compensation magnet will not fit into a launch vehicle fairing, it must be designed to deploy into an expanded state after launch. For these reasons, and others, discussed below, a preliminary pathfinder mission will be necessary to verify key designs.

3.2 Instrumentation

The NGS detector systems will be located on the cold side of the spacecraft's sunshield, as shown in Figure 1. The overall architecture is symmetrical and cylindrical, which provides a very large solid angle acceptance - see Figure 4. The solenoid magnet is wrapped with scintillating fiber (SciFi) trackers and time-of-flight (TOF) counters. The interior contains additional nested layers of TOF counters and SciFi trackers. The primary interior tracking duties are handled by silicon-strip detectors. At the core of the magnet is a cylindrical calorimeter with a pre-shower counter. Both payload endcaps are instrumented with SciFi Trackers and TOF counters. The endcap opposite to the service module has, in addition, a photon converter to allow the reconstruction of low-energy photons with good angular resolution. These converters consist of silicon detector layers interleaved with thin tungsten layers, as proposed for GAMMA-400 [66].

3.2.1 Tracking

NGS will have two types of tracking detector. On the exterior of the solenoid, there is a 3-layer high-resolution scintillating fiber tracker[67, 68], with a single point resolution of 40 µm. A second 3-layer SciFi tracker is located inside the solenoid. These sub-detectors provide rapid information on incoming particles, as undistorted by instrument interactions as possible.

The inner detector consists of a silicon tracker, similar in design to the AMS-02 silicon tracker [69]. It consists of six double layers arranged in a cylindrical geometry, leading to a maximum of 24 measurement points for a single track. The silicon tracker is assumed to have a single point resolution of 5 µm in the bending plane for $Z = 1$ particles. When combined with the 4 m diameter of the magnet and the magnetic field of 1 T, the NGS silicon tracker provides a maximum detectable rigidity of 100 TV, over an effective geometry of 100 m^2sr.

The NGS silicon tracker is of the same scale as the CMS barrel silicon tracker [70], which has an outer radius of 1.2 m and consists of 10 layers. Hence there is an existence proof for a detector with similar complexity. R&D drivers here include thermo-mechanical stability, and space certification.

3.2.2 Time of Flight

To reconstruct particle masses and thus identify isotopes in cosmic rays, a high-performance TOF system is required. Such systems, achieving time resolutions of 30ps to 50ps, are presently

under construction for the CMS and PANDA detectors [71, 72]. We assume here that the time resolution of the PANDA TOF, which employs a barrel structure of scintillator rods read out by SiPMs, can be significantly improved upon by instrumenting a larger fraction of the rod faces, and by running the SiPMs at 200 K, which allows for higher photon detection efficiencies. For $Z = 1$ particles, we target a time resolution of 20 ps for a single scintillator rod, leading to an overall time resolution of 15 ps for the 4-layer ToF system. This is clearly an area where detector R&D will have to be performed.

3.2.3 Calorimetery

A pre-shower detector and Lutetium-Yttrium oxyorthosilicate (LYSO) crystal calorimeter [73] are located at the center of the magnet solenoid. Together, they are used to separate electromagnetic and hadronic showers, and to measure the energy of electrons, positrons and photons, as well as protons and ions beyond the spectrometer's MDR. The inner calorimeter has an outer radius of 40 cm and is inspired by the design of the HERD detector [73]. Its unique 'cubic' voxel design provides acceptance at all azimuth angles, achieving a total geometric factor of 30 m^2sr, and allowing for the three-dimensional reconstruction of the shower shape.

The pre-shower detector consists of 12 silicon detector layers interleaved with thin tungsten sheets to provide good angular resolution for the measurement of γ rays, and to limit the back-splash of the calorimeter into the main silicon tracker. This combination of pre-shower detector and crystal calorimeter has a depth of $70\,X_0$, or $4\,\lambda_I$, for particles incident in the bending plane of the main solenoid and hitting the calorimeter centrally. The geometrical acceptance of this system allows the measurement of nuclei up to the cosmic-ray knee, at the PeV scale. Technical drivers similar to the TOF apply to the calorimeter.

3.3 Spacecraft Requirements

The NGS instrument will be installed on a satellite platform and operated for 10+ years at Lagrange Point 2. As discussed above, this positioning is necessary to provide the stable cold environment required for the operation of the HTS magnet behind a sunshield. In addition, the lower magnetic field in this region allows for attitude control which would not be possible in, e.g., a low-earth orbit, due to the interaction of the residual magnetic moment with the geomagnetic field. Finally, the shadow of the Earth would reduce the field of view and the geomagnetic cutoff would limit the sensitivity to low-energy cosmic antimatter, in particular to antideuterons from dark matter annihilations.

The instrumentation described above has a mass of ~ 43 tons (dominated by the calorimeter) and hence will require new heavy-lift launch capabilities, such as the NASA's Space Launch System (SLS)[74], which has been under development since 2011. The SLS Evolved Lift Capability program, aka Block 2, promises to support trans-lunar-injection launches of this mass or higher by 2030[75].

Sunshield The sunshield is a key component of NGS, allowing the HTS magnet to operate without cryogens. It has a radius 9 m and is designed similar to the concept developed for the JWST[76]. The dimensions of the sunshield are chosen such that a pointing accuracy of a few degrees towards the Sun is sufficient to keep the magnet system cool. Other than for thermal reasons, the orientation of the instrument has no impact on the physics program. Star trackers

will be used to monitor the orientation to provide precision information for the γ-ray astronomy program.

Data and Power Though the Deep Space Network has set targets for future Ka-band L2 downlink throughputs of up to 150 Mbps[77, 78], reducing the $\sim$MHz trigger rate of incoming particles to a level compatible with this downlink capacity will be a major challenge. To overcome it, the fast information provided by the outer detectors (i.e., TOF and SciFi-tracker), in combination with calorimeter measurements, will be used to generate smart trigger decisions. For example, light nuclei with rigidity below 100 GV will have to be mostly rejected. Prescaled random triggers will be used to estimate the related trigger efficiencies. In addition, exterior TOF and SciFi counters will be used to veto charged particles when reconstructing γ rays.

Power consumption of the payload is estimated to be 15kW, which will be provided by solar arrays.

4 Cost and Schedule

The NGS project is in an early phase, and hence full cost studies have not yet been performed. Nevertheless, we expect that the mission will fall into the Astro2020 'Large' category for space missions, implying a total (instrument+spacecraft+operations) cost of greater than $1.5B. Due to the technical complexity of the mission, it is clear that a pathfinder mission will be required, similar to that of LISA. The goal of the pathfinder mission will be to demonstrate, at L2, the stable operation of a high temperature superconducting magnet in space for the first time, including the expandable compensation coil technology, verify thermo-mechanical designs, as well as to verify detector designs and performance.

Research and Development	2019 - 2021
Technical Design Report	2020 - 2022
Pathfinder Construction	2023 - 2028
Pathfinder Launch	2029
Pathfinder Science Ops	2030 - 2036
NGS Construction	2031 - 2038
NGS Launch	2039
NGS Science Ops	2040 - 2050

Table 1: Schedule for the NGS project.

At a fraction of the full instrument size, and with a shorter operational lifetime, the pathfinder falls into the Astro2020 'Small' category for space missions, with an estimated total cost under $500M. A timeline of the various R&D and mission phases can be found in table 1.

An international consortium is currently forming to pursue the NGS concept. A similar white paper to this one will be submitted in August 2019 for the Voyage 2050 long-term plan in the ESA Science Program. We strongly encourage the agencies to consider long term research objectives of this scale, as international research projects. The very successful LHC experiments at CERN are an excellent role model for this approach.

With this white paper, we invite contributions from groups interested in participating in the project and encourage the community to support initial funding for the R&D stage of the mission, which we consider of the highest priority for future progress in astroparticle physics. Consider that the NGS concept, as outlined here and in [7], has the potential to improve on the sensitivity of the ground-breaking AMS-02 by a factor of 1000. This means that within the first week of operations, we will reproduce 20 years of AMS-02 data. In the second week, we will begin exploring completely new territory in precision astroparticle physics.

References

[1] P. Picozza et al. "PAMELA: A Payload for Antimatter Matter Exploration and Light-nuclei Astrophysics". In: *Astropart. Phys.* 27 (2007), pp. 296–315. DOI: 10.1016/j.astropartphys.2006.12.002. arXiv: astro-ph/0608697 [astro-ph].

[2] Andrei Kounine. "The Alpha Magnetic Spectrometer on the International Space Station". In: *International Journal of Modern Physics E* 21.8, 1230005 (Aug. 2012), p. 1230005. DOI: 10.1142/S0218301312300056.

[3] W. B. Atwood et al. "The Large Area Telescope on the Fermi Gamma-Ray Space Telescope Mission". In: ApJ 697 (June 2009), pp. 1071–1102. DOI: 10.1088/0004-637X/697/2/1071. arXiv: 0902.1089 [astro-ph.IM].

[4] S. C. C. Ting. "Latest Results from the AMS Experiment on the International Space Station". presented in the CERN Colloquium on 24th May 2018. 2018. URL: https://cds.cern.ch/record/2320166.

[5] Fabio Gargano. "The DAMPE experiment: 2 year in orbit". In: *Journal of Physics Conference Series*. Vol. 934. Dec. 2017, p. 012015. DOI: 10.1088/1742-6596/934/1/012015.

[6] O. Adriani et al. "The CALorimetric Electron Telescope (CALET) for high-energy astroparticle physics on the International Space Station". In: *Journal of Physics Conference Series*. Vol. 632. Aug. 2015, p. 012023. DOI: 10.1088/1742-6596/632/1/012023.

[7] S. Schael et al. "AMS-100: The Next Generation Magnetic Spectrometer in Space: An International Science Platform for Physics and Astrophysics at Lagrange Point 2". In: *NIM A* (2019, submitted). arXiv: 1907.04168 [astro-ph.IM].

[8] M. Rybczyński, Z. Włodarczyk, and G. Wilk. "Are there strangelets in cosmic rays?" In: *International Journal of Modern Physics A* 20.29 (2005), pp. 6724–6726. DOI: 10.1142/S0217751X05029939.

[9] M. Tanabashi et al. "Review of Particle Physics". In: *Phys. Rev. D* 98 (3 Aug. 2018), p. 030001. DOI: 10.1103/PhysRevD.98.030001.

[10] H. Fuke et al. "Search for fractionally charged particles in cosmic rays with the BESS spectrometer". In: *Advances in Space Research* 41.12 (2008), pp. 2050–2055. ISSN: 0273-1177. DOI: 10.1016/j.asr.2007.02.042.

[11] S. W. Hawking. "Particle creation by black holes". In: *Comm. Math. Phys.* 43.3 (1975), pp. 199–220. DOI: 10.1007/BF02345020.

[12] K. Maki, T. Mitsui, and S. Orito. "Local Flux of Low-Energy Antiprotons from Evaporating Primordial Black Holes". In: *Phys. Rev. Lett.* 76 (19 May 1996), pp. 3474–3477. DOI: 10.1103/PhysRevLett.76.3474.

[13] G. Amelino-Camelia et al. "Tests of quantum gravity from observations of γ-ray bursts". In: *Nature* 393.6687 (1998), pp. 763–765. DOI: 10.1038/31647.

[14] S. Agostinelli et al. "GEANT4: A simulation toolkit". In: *Nucl. Instrum. Meth. A* 506 (2003), pp. 250–303. DOI: 10.1016/S0168-9002(03)01368-8.

[15] M. Aguilar et al. "Precision Measurement of the Proton Flux in Primary Cosmic Rays from Rigidity 1 GV to 1.8 TV with the Alpha Magnetic Spectrometer on the International Space Station". In: *Phys. Rev. Lett.* 114.17 (Apr. 2015), p. 171103. ISSN: 1079-7114. DOI: 10.1103/physrevlett.114.171103.

[16] O. Adriani et al. "PAMELA Measurements of Cosmic-Ray Proton and Helium Spectra". In: *Science* 332 (2011), p. 69. DOI: 10.1126/science.1199172.

[17] M. Aguilar et al. "Observation of the Identical Rigidity Dependence of He, C, and O Cosmic Rays at High Rigidities by the Alpha Magnetic Spectrometer on the International Space Station". In: *Phys. Rev. Lett.* 119 (25 Dec. 2017), p. 251101. DOI: 10.1103/PhysRevLett.119.251101.

[18] M. Aguilar et al. "Towards Understanding the Origin of Cosmic-Ray Positrons". In: *Phys. Rev. Lett.* 122 (4 Jan. 2019), p. 041102. DOI: 10.1103/PhysRevLett.122.041102.

[19] Paolo Lipari. "Interpretation of the cosmic ray positron and antiproton fluxes". In: *Phys. Rev.* D95.6 (2017), p. 063009. DOI: 10.1103/PhysRevD.95.063009.

[20] R. Cowsik, B. Burch, and T. Madziwa-Nussinov. "The origin of the spectral intensities of cosmic-ray positrons". In: *Astrophys. J.* 786 (2014), p. 124. DOI: 10.1088/0004-637X/786/2/124.

[21] Kfir Blum, Boaz Katz, and Eli Waxman. "AMS-02 Results Support the Secondary Origin of Cosmic Ray Positrons". In: *Phys. Rev. Lett.* 111.21 (2013), p. 211101. DOI: 10.1103/PhysRevLett.111.211101.

[22] Yutaka Fujita et al. "Is the PAMELA anomaly caused by the supernova explosions near the Earth?" In: *Phys. Rev.* D80 (2009), p. 063003. DOI: 10.1103/PhysRevD.80.063003.

[23] Pasquale D. Serpico. "Astrophysical models for the origin of the positron 'excess'". In: *Astropart. Phys.* 39-40 (2012), pp. 2–11. DOI: 10.1016/j.astropartphys.2011.08.007.

[24] Tim Linden and Stefano Profumo. "Probing the Pulsar Origin of the Anomalous Positron Fraction with AMS-02 and Atmospheric Cherenkov Telescopes". In: *Astrophys. J.* 772 (2013), p. 18. DOI: 10.1088/0004-637X/772/1/18.

[25] P. Mertsch and S. Sarkar. "AMS-02 data confront acceleration of cosmic ray secondaries in nearby sources". In: *Physical Review D* 90.6 (2014), p. 061301. DOI: 10.1103/PhysRevD.90.061301.

[26] Nicola Tomassetti and Fiorenza Donato. "The Connection Between the Positron Fraction Anomaly and the Spectral Features in Galactic Cosmic-Ray Hadrons". In: *Astrophys. J.* 803.2 (2015), p. L15. DOI: 10.1088/2041-8205/803/2/L15.

[27] Dan Hooper et al. "HAWC Observations Strongly Favor Pulsar Interpretations of the Cosmic-Ray Positron Excess". In: *Phys. Rev.* D96.10 (2017), p. 103013. DOI: 10.1103/PhysRevD.96.103013.

[28] Wei Liu et al. "Excesses of Cosmic Ray Spectra from A Single Nearby Source". In: *Phys. Rev.* D96.2 (2017), p. 023006. DOI: 10.1103/PhysRevD.96.023006.

[29] M. Kachelrieß, A. Neronov, and D. V. Semikoz. "Cosmic ray signatures of a 2-3 Myr old local supernova". In: *Phys. Rev.* D97.6 (2018), p. 063011. DOI: 10.1103/PhysRevD.97.063011. arXiv: 1710.02321 [astro-ph.HE].

[30] Stefano Profumo et al. "Lessons from HAWC pulsar wind nebulae observations: The diffusion constant is not a constant; pulsars remain the likeliest sources of the anomalous positron fraction; cosmic rays are trapped for long periods of time in pockets of inefficient diffusion". In: *Phys. Rev.* D97.12 (2018), p. 123008. DOI: 10.1103/PhysRevD.97.123008.

[31] Michael S. Turner and Frank Wilczek. "Positron Line Radiation from Halo WIMP Annihilations as a Dark Matter Signature". In: *Phys. Rev.* D42 (1990), pp. 1001–1007. DOI: 10.1103/PhysRevD.42.1001.

[32] John R. Ellis. "Particles and cosmology: Learning from cosmic rays". In: *AIP Conf. Proc.* 516.1 (2000), p. 21. DOI: 10.1063/1.1291467.

[33] Hsin-Chia Cheng, Jonathan L. Feng, and Konstantin T. Matchev. "Kaluza-Klein dark matter". In: *Phys. Rev. Lett.* 89 (2002), p. 211301. DOI: 10.1103/PhysRevLett.89.211301.

[34] Marco Cirelli et al. "Model-independent implications of the e+-, anti-proton cosmic ray spectra on properties of Dark Matter". In: *Nucl. Phys. B* 813 (2009). [Addendum: Nucl. Phys. B 873 (2013) 530], pp. 1–21. DOI: 10.1016/j.nuclphysb.2008.11.031.

[35] Gordon Kane, Ran Lu, and Scott Watson. "PAMELA Satellite Data as a Signal of Non-Thermal Wino LSP Dark Matter". In: *Phys. Lett.* B681 (2009), pp. 151–160. DOI: 10.1016/j.physletb.2009.09.053.

[36] Joachim Kopp. "Constraints on dark matter annihilation from AMS-02 results". In: *Phys. Rev.* D88 (2013), p. 076013. DOI: 10.1103/PhysRevD.88.076013.

[37] Chuan-Hung Chen, Cheng-Wei Chiang, and Takaaki Nomura. "Dark matter for excess of AMS-02 positrons and antiprotons". In: *Phys. Lett.* B747 (2015), pp. 495–499. DOI: 10.1016/j.physletb.2015.06.035.

[38] Hsin-Chia Cheng et al. "AMS-02 Positron Excess and Indirect Detection of Three-body Decaying Dark Matter". In: *JCAP* 1703.03 (2017), p. 041. DOI: 10.1088/1475-7516/2017/03/041.

[39] Yang Bai, Joshua Berger, and Sida Lu. "Supersymmetric Resonant Dark Matter: a Thermal Model for the AMS-02 Positron Excess". In: *Phys. Rev.* D97.11 (2018), p. 115012. DOI: 10.1103/PhysRevD.97.115012.

[40] O. Adriani et al. "Cosmic-Ray Positron Energy Spectrum Measured by PAMELA". In: *Phys. Rev. Lett.* 111 (8 Aug. 2013), p. 081102. DOI: 10.1103/PhysRevLett.111.081102.

[41] F. Aharonian et al. "Probing the ATIC peak in the cosmic-ray electron spectrum with H.E.S.S." In: *Astronomy and Astrophysics* 508 (Dec. 2009), pp. 561–564. DOI: 10.1051/0004-6361/200913323.

[42] A. Archer et al. "Measurement of cosmic-ray electrons at TeV energies by VERITAS". In: Phys. Rev. D 98.6, 062004 (Sept. 2018), p. 062004. DOI: 10.1103/PhysRevD.98.062004. arXiv: 1808.10028 [astro-ph.HE].

[43] G. Ambrosi et al. "Direct detection of a break in the teraelectronvolt cosmic-ray spectrum of electrons and positrons". In: *Nature* 552 (2017), pp. 63–66. DOI: 10.1038/nature24475.

[44] M. Aguilar et al. "Precision Measurement of Cosmic-Ray Nitrogen and its Primary and Secondary Components with the Alpha Magnetic Spectrometer on the International Space Station". In: *Phys. Rev. Lett.* 121 (5 July 2018), p. 051103. DOI: 10.1103/PhysRevLett.121.051103.

[45] M. Korsmeier, F. Donato, and N. Fornengo. "Prospects to verify a possible dark matter hint in cosmic antiprotons with antideuterons and antihelium". In: *Physical Review D* 97.10 (May 2018), p. 103011. DOI: 10.1103/physrevd.97.103011.

[46] Su-Jie Lin, Xiao-Jun Bi, and Peng-Fei Yin. "Expectations of the Cosmic Antideuteron Flux". In: *arXiv e-prints* (Jan. 2018). arXiv: 1801.00997 [astro-ph.HE].

[47] M. Aguilar et al. "Antiproton Flux, Antiproton-to-Proton Flux Ratio, and Properties of Elementary Particle Fluxes in Primary Cosmic Rays Measured with the Alpha Magnetic Spectrometer on the International Space Station". In: *Phys. Rev. Lett.* 117.9 (Aug. 2016), p. 091103. ISSN: 1079-7114. DOI: 10.1103/physrevlett.117.091103.

[48] M. Aguilar et al. "Electron and Positron Fluxes in Primary Cosmic Rays Measured with the Alpha Magnetic Spectrometer on the International Space Station". In: *Phys. Rev. Lett.* 113.12, 121102 (2014), p. 121102. DOI: 10.1103/PhysRevLett.113.121102.

[49] K. Abe et al. "Measurement of the Cosmic-Ray Antiproton Spectrum at Solar Minimum with a Long-Duration Balloon Flight over Antarctica". In: *Phys. Rev. Lett.* 108.5, 051102 (Feb. 2012), p. 051102. DOI: 10.1103/PhysRevLett.108.051102.

[50] Fiorenza Donato, Nicolao Fornengo, and Pierre Salati. "Antideuterons as a signature of supersymmetric dark matter". In: *Phys. Rev. D* 62 (4 July 2000), p. 043003. DOI: 10.1103/PhysRevD.62.043003. URL: https://link.aps.org/doi/10.1103/PhysRevD.62.043003.

[51] Y. Cui, J. D. Mason, and L. Randall. "General analysis of antideuteron searches for dark matter". In: *Journal of High Energy Physics* 2010.11 (Nov. 2010), p. 17. ISSN: 1029-8479. DOI: 10.1007/JHEP11(2010)017.

[52] H. Fuke et al. "Search for Cosmic-Ray Antideuterons". In: *Phys. Rev. Lett.* 95 (8 Aug. 2005), p. 081101. DOI: 10.1103/PhysRevLett.95.081101.

[53] Pascal Chardonnet, Jean Orloff, and Pierre Salati. "The production of anti-matter in our galaxy". In: *Physics Letters B* 409.1 (1997), pp. 313–320. DOI: 10.1016/S0370-2693(97)00870-8.

[54] J. A. Hinton and W. Hofmann. "Teraelectronvolt astronomy". In: *Ann. Rev. Astron. Astrophys.* 47 (2009), pp. 523–565. DOI: 10.1146/annurev-astro-082708-101816.

[55] F. A. Aharonian. "Gamma rays from supernova remnants". In: *Astroparticle Physics* 43 (2013), pp. 71–80. DOI: https://doi.org/10.1016/j.astropartphys.2012.08.007.

[56] S. Funk. "High-Energy Gamma Rays from Supernova Remnants". In: *Handbook of Supernovae*. Ed. by Athem W. Alsabti and Paul Murdin. Cham: Springer International Publishing, 2017, pp. 1737–1750. ISBN: 978-3-319-21846-5. DOI: 10.1007/978-3-319-21846-5_12.

[57] B. M. Gaensler and P. O. Slane. "The Evolution and Structure of Pulsar Wind Nebulae". In: *Ann. Rev. Astron. Astrophys.* 44 (Sept. 2006), pp. 17–47. DOI: 10.1146/annurev.astro.44.051905.092528.

[58] B. S. Acharya et al. "Introducing the CTA concept". In: *Astroparticle Physics* 43 (2013), pp. 3–18. DOI: 10.1016/j.astropartphys.2013.01.007.

[59] V. Selvamanickam et al. "High Performance 2G Wires: From R&D to Pilot-Scale Manufacturing". In: *IEEE Transactions on Applied Superconductivity* 19.3 (June 2009), pp. 3225–3230. ISSN: 1051-8223. DOI: 10.1109/TASC.2009.2018792.

[60] C. Senatore et al. "Progresses and challenges in the development of high-field solenoidal magnets based on RE123 coated conductors". In: *Superconductor Science and Technology* 27.10 (Sept. 2014), p. 103001. DOI: 10.1088/0953-2048/27/10/103001.

[61] T. Benkel et al. "REBCO tape performance under high magnetic field". In: *Eur. Phys. J. Appl. Phys.* 79.3 (2017), p. 30601. DOI: 10.1051/epjap/2017160430.

[62] C. Barth, G. Mondonico, and C. Senatore. "Electro-mechanical properties of REBCO coated conductors from various industrial manufacturers at 77 K, self-field and 4.2 K, 19 T". In: *Superconductor Science and Technology* 28.4 (Feb. 2015), p. 045011. DOI: 10.1088/0953-2048/28/4/045011.

[63] K. Ilin et al. "Experiments and FE modeling of stress-strain state in ReBCO tape under tensile, torsional and transverse load". In: *Superconductor Science and Technology* 28.5 (Mar. 2015), p. 055006. DOI: 10.1088/0953-2048/28/5/055006.

[64] M. Daibo (Fujikura). *Recent Progress of 2G HTS wires and coils at Fujikura*. presentation at Workshop on Advanced Superconducting Materials and Magnets, Jan. 2019, KEK, Japan. 2019. URL: https://conference-indico.kek.jp/indico/event/62/contribution/22/material/slides/0.pdf.

[65] M. Bonura and C. Senatore. "An equation for the quench propagation velocity valid for high field magnet use of REBCO coated conductors". In: *Applied Physics Letters* 108.24 (2016), p. 242602. DOI: 10.1063/1.4954165.

[66] A. M. Galper, N. P. Topchiev, and Yu. T. Yurkin. "GAMMA-400 Project". In: *Astronomy Reports* 62.12 (Dec. 2018), pp. 882–889. ISSN: 1562-6881. DOI: 10.1134/S1063772918120223.

[67] B. Beischer et al. "A high-resolution scintillating fiber tracker with silicon photomultiplier array readout". In: *Nucl. Instrum. Meth. A* 622 (2010), pp. 542–554. DOI: 10.1016/j.nima.2010.07.059.

[68] Thomas Kirn. "SciFi – A large scintillating fibre tracker for LHCb". In: *Nucl. Instrum. Meth. A* 845 (2017). Proceedings of the Vienna Conference on Instrumentation 2016, pp. 481–485. ISSN: 0168-9002. DOI: 10.1016/j.nima.2016.06.057.

[69] J. Alcaraz et al. "The alpha magnetic spectrometer silicon tracker: Performance results with protons and helium nuclei". In: *Nucl. Instrum. Meth. A* 593.3 (Aug. 2008), pp. 376–398. ISSN: 0168-9002. DOI: 10.1016/j.nima.2008.05.015.

[70] S. Chatrchyan et al. "The CMS experiment at the CERN LHC". In: *Journal of Instrumentation* 3.08 (Aug. 2008), S08004–S08004. DOI: 10.1088/1748-0221/3/08/s08004.

[71] CMS Collaboration. *Technical Proposal For A MIP Timing Detector in the CMS Experiment Phase 2 Upgrade*. Tech. rep. CERN-LHCC-2017-027. LHCC-P-009. Geneva: CERN, Dec. 2017. URL: https://cds.cern.ch/record/2296612.

[72] PANDA Collaboration. *Technical Design Report for the PANDA Barrel TOF*. Tech. rep. GSI, 2018. URL: https://panda.gsi.de/system/files/user_uploads/ken.suzuki/RE-TDR-2016-003_0.pdf.

[73] S. N. Zhang et al. "The high energy cosmic-radiation detection (HERD) facility onboard China's Space Station". In: *Proceedings of the SPIE*. Vol. 9144. 2014. DOI: 10.1117/12.2055280. eprint: 1407.4866.

[74] NASA. *Space Launch System*. 2019. URL: https://www.nasa.gov/exploration/systems/sls/index.html (visited on 06/27/2019).

[75] W. Gerstenmaier. *Progress in Defining the Deep Space Gateway and Transport Plan*. 2017. URL: https://www.nasa.gov/sites/default/files/atoms/files/nss_chart_v23_tagged.pdf (visited on 06/27/2019).

[76] J. Arenberg et al. "Status of the JWST sunshield and spacecraft". In: *Proc. SPIE 9904, Space Telescopes and Instrumentation 2016: Optical, Infrared, and Millimeter Wave*. 2016, p. 990405. DOI: 10.1117/12.2234481.

[77] Remi Labelle and David Rochblatt. "Ka-band high-rate telemetry system upgrade for the NASA deep space network". In: *Acta Astronautica - ACTA ASTRONAUT* 70 (Feb. 2012). DOI: 10.1016/j.actaastro.2011.07.023.

[78] B. Younes. *Future of Space Communications*. 2012. URL: https://www.nasa.gov/pdf/696855main_Pres_Future_of_Space_Communications_SGC_2012.pdf (visited on 06/27/2019).